Characterization of the anion-ordering transition in $(TMTTF)_2ReO_4$ by x-ray absorption and photoemission spectroscopies

G. Subías
Instituto de Ciencia de Materiales de Aragón (ICMA), Departamento de Física de la Materia Condensada, CSIC-Universidad de Zaragoza, Pza. San Francisco s/n, E-50009 Zaragoza, Spain

T. Abbaz and J. M. Fabre
Institut Charles Gerhardt, UMR CNRS 5253, AM2N, ENSCM, 8 rue de l' École Normale, F-34296 Montpellier cedex 5, France

J. Fraxedas*
Institut de Ciència de Materials de Barcelona (ICMAB-CSIC), Campus de la UAB, E-08193 Bellaterra, Spain
(Received 4 May 2007; revised manuscript received 18 June 2007; published 3 August 2007)

We have characterized the electronic structure of single crystals of the organic quasi-one-dimensional salt $(TMTTF)_2ReO_4$ (TMTTF=tetramethyl-tetrathiafulvalene) by x-ray-absorption near-edge spectroscopy and x-ray photoemission spectroscopy using synchrotron radiation under low-intensity conditions (single-bunch ring operation mode) in order to strongly reduce detrimental beam-induced damage. The observed differences in spectra taken at $T=116$ K and $T=207$ K are ascribed to the anion-ordering transition, which takes place at 155 K. It is proposed that the ordering transition driven by the anions perturbs the structural organization of the organic stacks, increasing the overlap of the π-type orbitals through dimerization.

DOI: 10.1103/PhysRevB.76.085103 PACS number(s): 71.20.−b, 71.30.+h, 78.70.Dm, 79.60.−i

I. INTRODUCTION

The family of the isostructural quasi-one-dimensional organic mixed-valence radical cation salts $(TMTTF)_2X$ and $(TMTSF)_2X$ based on the π donors TMTTF (tetramethyl-tetrathiafulvalene) and TMTSF (tetramethyl-tetraselenafulvalene), where X stands for a monovalent anion (PF_6^-, ClO_4^-, ReO_4^-, etc.), exhibits complex and extremely rich phase diagrams with a variety of ground states (metallic, Mott-Hubbard, spin-Peierls, antiferromagnetic, spin and charge density wave, and superconducting). Such unusual wealth of competing electronic and structural instabilities, which gives rise to a fascinating low-dimensional physics, continues to attract materials chemists and physicists after more than 25 years, these salts, known as the Bechgaard-Fabre salts, becoming intensively studied reference systems.[1–8]

The crystal structure of such salts consists of nearly uniform stacks of TMTTF or TMTSF molecules, aligned along the crystallographic a axis, the conduction axis, ordered in sheets separated by anion sheets, which can be regarded as organic and inorganic superlattices. When grown by constant low dc oxidation of an organic solution of the corresponding neutral donor molecule and tetrabutyl ammonium salt of the anion as electrolyte,[9] the Bechgaard-Fabre salts crystallize in the triclinic $P\bar{1}$ space group.[10,11] However, they have been found to order in the monoclinic $C2/c$ space group when prepared under different experimental conditions, i.e., by confined electrocrystallization.[12] Figure 1 shows the room-temperature structure of the triclinic phase of the title compound $(TMTTF)_2ReO_4$.[13]

The monovalent anions can be either centrosymmetric or noncentrosymmetric. Those salts with noncentrosymmetric anions, such as, e.g., ClO_4^- and ReO_4^-, exhibit anion ordering below a given temperature. Above the transition temperature T_{AO}, the anions exhibit random orientations but for sufficiently low temperatures they become ordered. The anion-ordering transition has important consequences on the low-temperature properties and ground states of these materials. When the period along a is doubled, the anion potential can open an energy gap at the Fermi level E_F, thus inducing a metal-insulator transition.[14]

TMTTF salts with centrosymmetric anions exhibit charge-ordering phase transitions.[15,16] In this case no structural modifications have been observed for these salts along the transition, hence deserving the term structureless. Upon charge ordering the electronic equivalence of the TMTTF molecules is removed below a critical temperature, making the charge disproportionate.

Let us now concentrate on the title compound. For $(TMTTF)_2ReO_4$, where ReO_4^- has a tetrahedral symmetry, the room-temperature conductivity is about 25 Ω^{-1} cm^{-1}.[13,17,18] The temperature dependences of the electrical resistance and of the thermopower show two anomalies near 225 K and 160 K.[19] In addition, the dielectric constant measured at 6.5 GHz presents also two anomalies near the same temperatures.[20] The 160 K feature is due to anion ordering, as revealed by x-ray studies, showing a superstructure represented by the reduced wave vector $(\frac{1}{2}\frac{1}{2}\frac{1}{2})$, leading to the opening of an energy gap at E_F.[21] The transition near 225 K is due to charge ordering with a ferroelectric character, as suggested by low-frequency conductivity and dielectric permittivity measurements.[18,22]

Here we study the electronic structure of triclinic $(TMTTF)_2ReO_4$ by means of x-ray-absorption near-edge spectroscopy (XANES) and x-ray photoemission spectroscopy (XPS) with synchrotron radiation with special emphasis on the anion-ordering transition. XANES yields information on unoccupied states, and being sensitive to bond-angles, linearly polarized x rays are best suited for molecules pos-

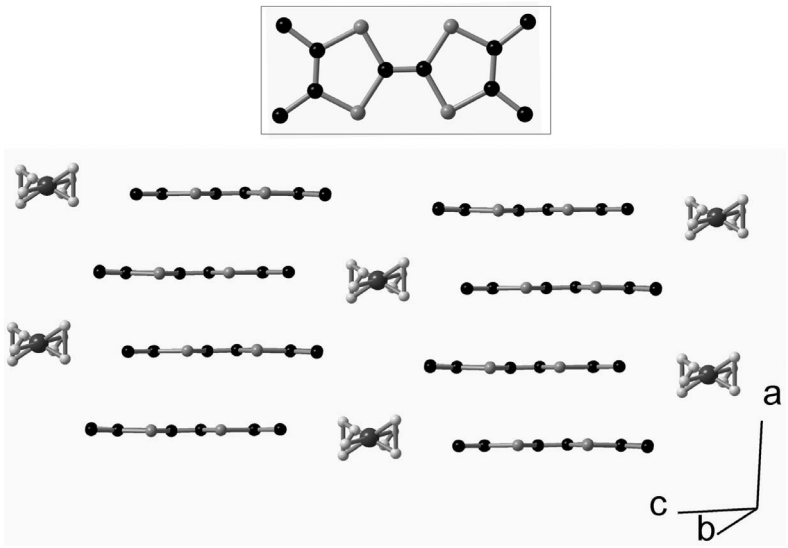

FIG. 1. View of the crystal structure of triclinic $(TMTTF)_2ReO_4$ at 293 K. C, Re, S, and O atoms are represented by black, dark gray, medium gray, and light gray balls, respectively. H atoms are omitted for clarity. The two disordered positions of the anions are represented. The inset shows a TMTTF molecule along the *a* axis.

sessing directional bonds. This is best exemplified for π-conjugated molecules lying flat on surfaces. When the electric field vector **E** of the synchrotron light is aligned along the surface normal, features due to the out-of-plane π orbitals (antisymmetric with respect to the molecular plane) are seen, and when **E** is parallel to the surface, resonances due to the in-plane σ orbitals (symmetric with respect to the molecular plane) are dominant. By varying the angle between the incident beam and the substrate, the orientation of the molecules can be elucidated.[23] Apart from this purely geometrical constraint, dipolar selection rules also apply. According to these selection rules atomic levels with an orbital quantum number l can be excited only to those levels with $l\pm1$. Hence *s* initial states can only be excited to *p* final states, while from *p* the achievable final states are *s* and *d*.[24]

Previous XANES measurements on Fabre salts have been focused on the evaluation of charge ordering involving centrosymmetric anions. In the case of $(TMTTF)_2PF_6$ XANES experiments involving the S *K* edge (S 1*s*) show no evidence of charge disproportionation larger than 0.5 electrons/molecule, and extended x-ray-absorption fine structure (EXAFS) at the P *K* edge indicate no displacements of the PF_6 anion larger than 0.05 Å.[25] The *K* edge of sulfur has been used because its energy is very sensitive to the electronic oxidation state of sulfur involved in a molecule.[26] In our work we report XANES measurements of the S 2*p* states because XANES features for this *L* edge are more sensitive to the local bonding configurations than the corresponding *K*-edge features. Moreover, the unoccupied *d*-type electronic states can be well resolved, as reported on a previous investigation with the quasi-one-dimensional metal TTF-TCNQ [TTF=tetrathiafulvalene, TCNQ=tetracyanoquinodimethane].[27]

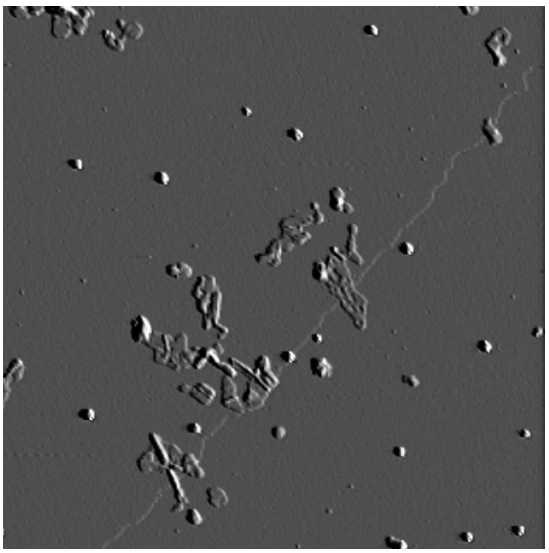

FIG. 2. Amplitude AFM image taken in tapping mode at ambient conditions of a (001) surface of a $(TMTTF)_2ReO_4$ single crystal. The diagonal line is due to a $\simeq$1.3-nm-high step ($\simeq c$). The scale is 5 μm$\times$5 μm.

II. EXPERIMENT

$(TMTTF)_2ReO_4$ single crystals were obtained by electrocrystallization carried out in a galvanostatic mode in a two-compartments U-shaped cell equipped with two platinum wires used as electrodes. Typical dimensions of the samples were $5\times0.5\times0.3$ mm^3. The samples were mounted on OFHC copper sample holders by gluing them with UHV silver epoxy and exposing the (001) face [*ab* plane], thus with the long axis (*a* axis) contained in the sampler holder's plane, in order to be able to align the *a* axis with the linear polarization vector **E** with the help of the polar and azimuthal rotations of the manipulator. Special care was taken not to break the crystals when mounting them on the holders due to their brittle nature. The single crystals are very stable both in air and in UHV so that they were measured *as received* in a base pressure in the low 10^{-9} mbar range. The reasons to avoid *in situ* surface preparation are on the one hand the small dimensions and brittle nature of the crystals, which prevents from cleaving the samples in UHV, and on the other hand that they cannot be prepared by traditional techniques such as ion sputtering. The exposed surfaces were indeed contaminated, as observed on the exploratory XPS

spectra, but in spite of that they were sufficiently clean and crystalline in order to perform XANES and XPS measurements. In a previous example of TTF-TCNQ the dispersion of the occupied bands near E_F could be obtained in *as received* samples.[28] Figure 2 shows a representative atomic force microscopy (AFM) image of the surface. The image evidences that most of the surface is clean. The defects observed are the result of the evaporation of the solvent.[29]

The XANES measurements were performed at the multiuser stage for angular-resolved photoemission (MUSTANG) endstation (dipole beamline PM3) of the *Berliner Elektronspeicherring für Synchrotronstrahlung* (BESSY) in Berlin, Germany. Since the Bechgaard-Fabre salts are known to be irreversibly damaged upon VUV and x-ray irradiation,[30,31] we have selected the single-bunch ring operation mode, thus reducing the photon beam intensity. The storage ring operates at 1.7 GeV and the maximum ring current was set to 20 mA during the single-bunch operation. Under these conditions we observed modifications in the spectra after approximately 24 h. On the other hand, the samples were measured always at low temperature, thus further reducing the beam-induced damage, and the radiation was stopped when spectra were not acquired (monochromator setting, change of temperature, etc.). In addition, the samples were cooled slowly (<1 K min^{-1}) in order to avoid the formation of cracks.[32] As a consequence of the chosen low-intensity conditions, the measurements become rather long, implying that the temperature-dependent experiments have to be performed for a few selected temperatures.

The data were acquired in the total electron yield mode. The experimental station is equipped with a Phoibos 150 hemispherical electron analyzer arranged at a fixed angle of 45° with respect to the incident beam and the electrons are detected by an array of nine channel electron multipliers at a fixed kinetic energy in the region of the secondary electron background (10 eV). The information on the spatial distribution of empty states has been obtained from XANES measurements at different angles of incidence, θ, of the x-ray light, performed by rotating the sample and taking advantage of the intrinsic linear polarization of synchrotron radiation. For $\theta=0$ and θ close to 90°, **E** lies parallel and perpendicular to the crystallographic *a* axis, respectively.

III. RESULTS AND DISCUSSION

Let us start with the XANES measurements concerning the organic donor TMTTF. Figure 3 shows the S $2p$ XANES spectra for $(TMTTF)_2ReO_4$ taken at 207 K and at different angles of incidence. This temperature is above the anion-ordering transition (near 160 K) but below the charge-ordering transition (near 255 K). The signal was normalized to the time-dependent variation of the intensity of synchrotron radiation and, then, to the experimental background measured in the same energy region from a freshly evaporated Ni film. The XANES spectra were finally normalized to the high-energy part of each spectrum for comparison purposes. The spectra exhibit two differentiated regions: a structured (discrete) one below ca. 170 eV photon energy due to

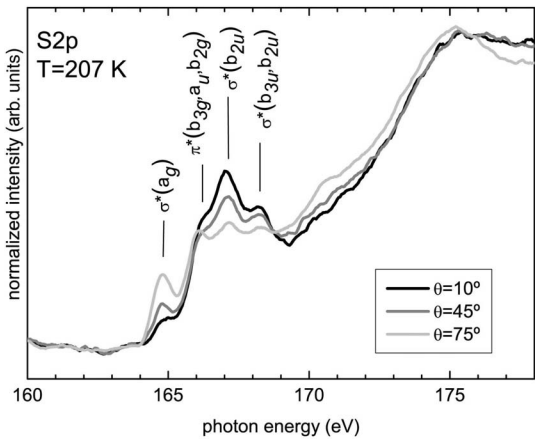

FIG. 3. Normalized S $2p$ XANES spectra for $(TMTTF)_2ReO_4$ taken at 207 K for $\theta=10°$ (solid black line), 45° (solid gray line) and 75° (solid light gray line).

unoccupied electronic states and an unstructured region above 170 eV associated with a continuum of electronic states. The spectra closely resemble the S $2p$ inelastic electron scattering spectra[33] and the S $2p$ XANES spectra of TTF-TCNQ,[27] as might be expected, since TTF is the core of TMTTF and the only difference between TTF and TMTTF is the presence of four methyl groups in the latter, which should have negligible contribution to the DOS.

Let us thus explore the origin of the observed structures below 170 eV. The symmetry labels adopted next are those appropriate for idealized D_{2h} symmetry and are based on a first-principles density functional theory (DFT) calculations performed on TTF-TCNQ[27] carried out using the SIESTA code.[34] According to such calculations, the C partial density of states (PDOS) is dominated by *p*-type contributions with *s*- and *d*-type contributions being much smaller, in the energy region up approximately 5–6 eV above E_F. However, for the S PDOS the weight of the *d*-type contributions become considerably larger. In fact, the *d* contributions extend over all the energy range of interest so that even if the *p* contributions dominate, there is always some *d* contribution of the appropriate symmetry.

The peak located at ~165 eV photon energy originates from the a_g orbital, a σ-type orbital. The main character is C-S antibonding, and this orbital will be labeled as $\sigma^*(a_g)$. The next structure, a shoulder at ~166 eV, originates from the contributions of b_{3g} orbitals and from the pair of a_u and b_{2g} orbitals, which are of π type. The associated feature will be labeled as $\pi^*(b_{3g},a_u,b_{2g})$ and is observed because of its significant *d* character. The next peak, located at ~167 eV, is due to b_{2u} orbitals and is another antibonding C-S level and will be labeled $\sigma^*(b_{2u})$. This orbital contains a sizable contribution of the appropriate symmetry-adapted combination of d_{z2} orbitals of the S atoms. This observation will be important in order to understand the angular dependence of the S $2p$ XANES spectra. The shoulder at ~168 eV originates from two orbitals of similar energy in the molecule: the b_{3u} and b_{2u} orbitals. These two orbitals are also C-S antibonding but include also some C-C antibonding character and will be termed as $\sigma^*(b_{3u},b_{2u})$.

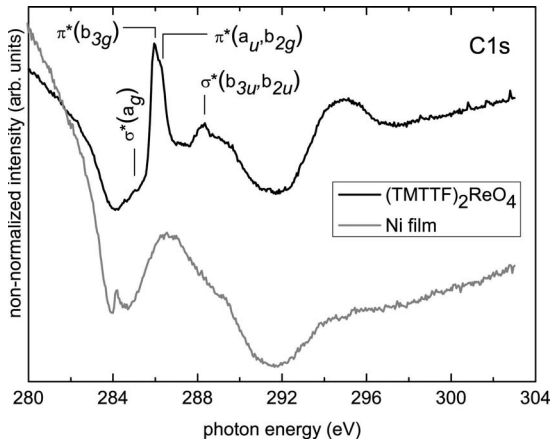

FIG. 4. C 1*s* XANES spectra of $(TMTTF)_2ReO_4$ taken at $\theta=45°$ and 207 K (solid black line) and of a freshly *in situ* grown Ni film (solid gray line).

The most relevant trends in Fig. 3 are the intensity reduction of the $\sigma^*(b_{2u})$ and the increase of $\sigma^*(a_g)$ with increasing θ. According to the geometry and orientation of the TMTTF molecules and their molecular orbitals, the absorption intensity should be maximum for σ-type orbitals when **E** coincides with the molecular plane—i.e., for large θ values. This is indeed observed for $\sigma^*(a_g)$ but not for $\sigma^*(b_{2u})$. The reason for this behavior is that, as pointed out earlier, the $\sigma^*(b_{2u})$ feature exhibits a significant d_{z2} contribution, an orbital pointing perpendicularly to the TMTTF molecular plane. The d_{z2} contribution to the XANES spectrum should be more evident for lower θ values and should be strongly reduced for large θ values, as experimentally observed. Similarly to the $\sigma^*(b_{2u})$ feature, $\pi(b_{3g},a_u,b_{2g})$ should decrease at larger θ values because of the orbital distribution. This behavior is not evident from the spectra because of the overlap with $\sigma^*(b_{2u})$ but the intensity ratio between $\pi(b_{3g},a_u,b_{2g})$ and $\sigma^*(a_g)$ decreases for increasing θ values, as expected.

The C 1*s* XANES spectra taken at $\theta=45°$ and measured at 207 K is shown in Fig. 4 (upper part) and compared to the background spectra corresponding to the freshly deposited Ni film (lower part). Both spectra are not normalized. From the comparison it becomes evident that important contributions from different optical components of the beamline, such as monochromator, mirrors, and slits, are at hand and for this reason we have not pursued a more detailed analysis. However, it is still possible to identify in the 284–292 eV energy window of interest specific XANES features related to the molecular orbitals of defined symmetry of the $(TMTTF)_2ReO_4$ sample, in agreement with those observed in the S 2*p* spectrum. The most prominent one, a peak centered at about 286 eV, corresponds to the $\pi^*(b_{3g},a_u,b_{2g})$ orbitals. Note that the peak can be resolved into two contributions: the lower photon energy contribution originates from the b_{3g} orbital and the shoulder at higher photon energy originates from the pair of a_u and b_{2g} orbitals, respectively. The calculated energy separation between a_u, b_{2g}, and b_{3g} for TTF is about 0.4 eV,[27] which is of the order of the separation found in the spectrum of Fig. 4. The less prominent feature, centered at 288.2 eV, can be associated with $\sigma^*(b_{3u},b_{2u})$ orbitals

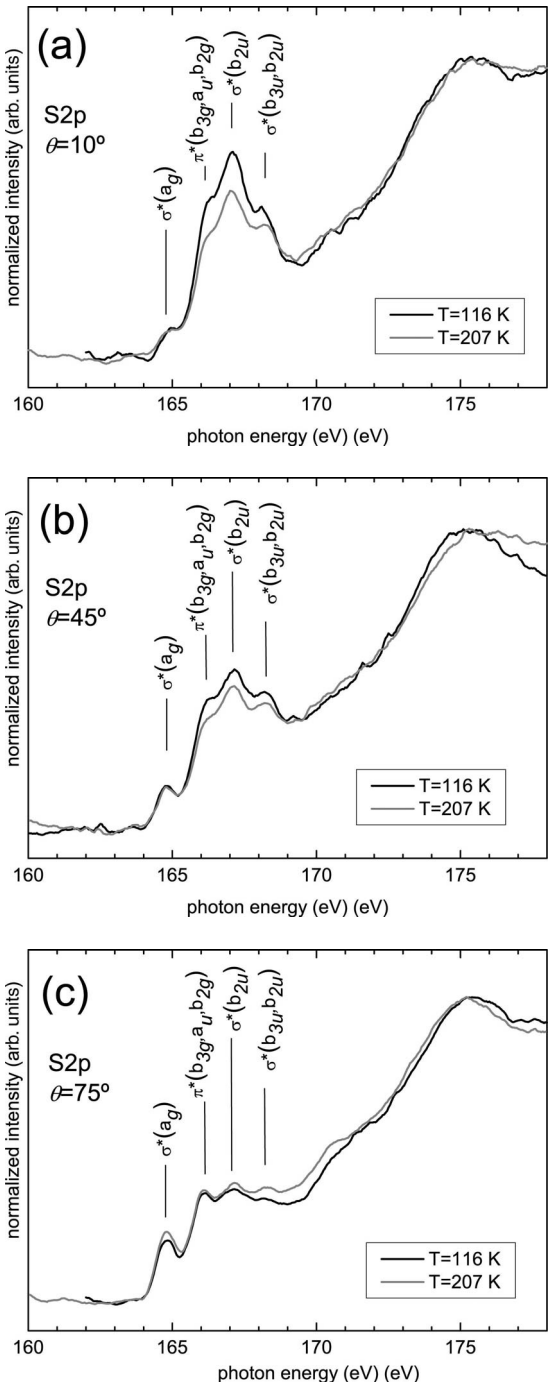

FIG. 5. Normalized S 2*p* XANES spectra for (a) $\theta=10°$, (b) $\theta=45°$, and (c) $\theta=75°$ taken at 116 (solid black line) and 207 K (solid gray line).

and the weak shoulder at 285 eV might be associated with $\sigma^*(a_g)$. Summarizing, both S 2*p* and C 1*s* XANES spectra allow us to determine the unoccupied DOS of the organic donor TMTTF.

Figure 5 shows the S 2*p* XANES spectra represented for (a) $\theta=10°$, (b) $\theta=45°$, and (c) $\theta=75°$ at 116 and 207 K. The temperature-dependent spectra reveal that the signal arising from $\sigma^*(a_g)$ is essentially insensitive to anion ordering while the features related to $\sigma^*(b_{2u})$, $\pi(b_{3g},a_u,b_{2g})$, and $\sigma^*(b_{3u},b_{2u})$ clearly increase upon undergoing the anion-

ordering transition. This effect is particularly evident for $\theta = 10°$ and to a lesser extent for $\theta = 45°$. Note that for $\theta = 75°$ both spectra are essentially unchanged. This suggests that anion ordering induces a reorganization of the molecular stacks, probably increasing the orbital overlap, since it affects mostly the π-type orbitals. In fact it has been established by means of x-ray diffraction studies that there is an important tetramerization of the TMTTF stacks below the transition temperature.[21]

In order to explore the influence of the transition on the anions, we have measured the O 1*s* XANES spectra at 116 and 207 K (not shown). In this case both spectra look identical, with two prominent peaks at 530.7 and 532.7 eV, respectively, so that we can conclude in view of the XANES results that the effect is negligible.[35]

Let us now discuss the high-resolution XPS measurements performed on the $(TMTTF)_2ReO_4$ samples. Figure 6(a) shows the XPS spectrum of the Re 4*f* line measured at 207 K with 600-eV photons. A least-squares fit to a function consisting in the product of a Gaussian and Lorentzian functions of the same width (solid line) satisfactorily reproduces the experimental curve (open circles). From the fit an asymmetry parameter $\alpha = 0.10$, a width $W = 0.37$ eV and a Lorentzian-Gaussian mixing ratio $M = 0.72$ are obtained for both Re $4f_{7/2}$ and Re $4f_{5/2}$ components. The fact that both spin-orbit components exhibit the same width is associated with the molecular character of the material, also evidenced in the discrete nature of the S 2*p* and C 1*s* XANES spectra, since a typical solid-state effect of materials containing 4*f* elements is an excess broadening of the high-energy spin-orbit component due to Coster-Kronig processes.[36] The observed asymmetry cannot be assigned to screening by the conduction electrons of the holes generated during the photoemission process, as those found in inorganic metals and in TTF-TCNQ,[31] since the data cannot be fitted using a Doniach-Šunjić function. The effect of contaminants should be observed as a component, and not just as an asymmetry, and would evolve with time, a fact that was not observed after more than 24 h. The potential presence of surface core level shifts (0.17 eV as determined in renium single crystals[37]) or any shifts associated to regions with different charging (i.e., separate crystals) should be also seen as components and not as asymmetric lines. On the other hand, the spurious contribution of the Re $5p_{3/2}$ line can be excluded since it overlaps only slightly in the low binding energy side of the Re $4f_{7/2}$ line. We believe that the observed asymmetry could be due to the Franck-Condon principle—that is, to inelastic scattering associated with vibrational excitations (phonons).[38]

In Fig. 6(b) both Re 4*f* XPS spectra measured at 116 and 207 K are compared, normalized to the peak maximum (Re $4f_{7/2}$). The 116-K spectrum has been shifted 0.17 eV towards lower binding energy in order to coincide with the 207-K spectrum. This shift may arise from the opening of an energy gap below the anion-ordering transition.[39] We observe, in particular from the difference spectrum (bottom of the figure), that the asymmetry α increases below the transition from 0.10 (207 K) to 0.13 (116 K), a small but reproducible and reversible change. From the difference spectrum a structure at 0.7 eV above the Re $4f_{7/2}$ peak position is obtained. This value seems too large to be assigned to the anion-ordering derived gap, i.e., through a shake-up satellite. The expected energy gap lies in the 0.1–0.2 eV range,[18] so that the 0.7 eV carries more information than the expected gap opening. The observed peaks shapes are reversible: when the temperature is increased up to 207 K, the initial spectrum is restored, so that we can eliminate any contribution from surface contaminants. In addition, charging can be excluded as the origin of the observed increase in asymmetry since the widths of the peaks remain essentially identical [compare in Fig. 6(b) the low binding energy sides of both 4*f* components at both temperatures]. On the other hand, such an increase in asymmetry cannot be due to the Franck-Condon principle, since the asymmetry increases at lower temperature, where the number of excited phonons is smaller.

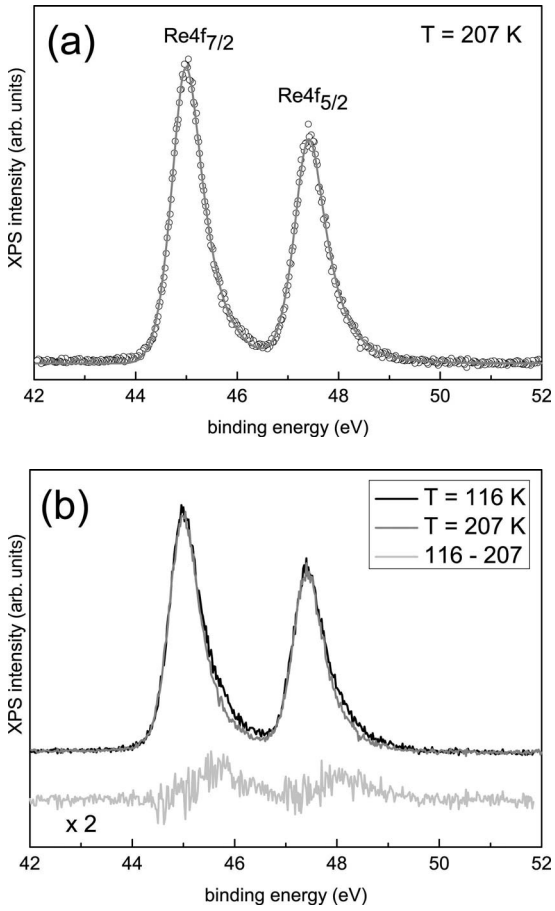

FIG. 6. (a) XPS Re 4*f* line measured at 207 K with 600 eV photons. The experimental spectrum (open circles) has been fitted to a Gaussian-Lorentzian product function (solid gray line) after a linear background subtraction with the resulting parameters: energy position of the Re $4f_{7/2}$ line $E = 45.0$ eV, spin-orbit splitting $S = 2.42$ eV, branching ratio $B = 0.75$, asymmetry parameter $\alpha = 0.10$, peak width $W = 0.37$, and Lorentzian-Gaussian mixing ratio $M = 0.72$. (b) Comparison of the XPS lines taken at 116 (solid black line) and 207 K (solid gray line). The fit parameters for the 116 K spectrum are $E = 45.17$ eV, $S = 2.42$ eV, $B = 0.75$, $\alpha = 0.13$, $W = 0.38$, and $M = 0.79$. The difference spectrum is shown at the bottom (solid light gray line).

Thus, the increase in asymmetry for $T < T_{AO}$ is associated with the anion-ordering transition, and it has to be related to small displacements and/or deformations of the perrhenate tetrahedra, as previously suggested,[21] which are undetected with the O 1*s* XANES signals.

IV. CONCLUSIONS

We have experimentally characterized the electronic structure of $(TMTTF)_2ReO_4$ by means of XANES and XPS in order to investigate the driving mechanism of the anion-ordering transition.

(i) Angular-dependent S 2*p* and C 1*s* XANES measurements allow us to assign experimental observed features to molecular orbitals of specific energy and symmetry. The unoccupied electronic levels closely resemble those previously reported for charged TTF in TTF-TCNQ.

(ii) Temperature-dependent S 2*p* XANES spectra show an increase in the intensity mostly for features associated with π-type or d_{z2} orbitals (i.e., perpendicular to the TMTTF molecular plane) upon undergoing the anion-ordering transition associated to an increase in orbital overlap.

(iii) No relevant changes are detected in the O 1*s* XANES spectra across the anion-ordering transition.

(iv) A small but reproducible increase in the asymmetry of the Re 4*f* XPS spectra is observed at temperatures below the AO transition, which we ascribe to small displacements and/or deformations of the ReO^-_4 tetrahedra.

Our results confirm the displacive character of the $(TMTTF)_2ReO_4$ anion-ordering transition as previously pointed out by Parkin, Mayerle, and Engler.[21]

ACKNOWLEDGMENTS

We are grateful to BESSY for granting beam time and to the BESSY staff for support during the experiment. We thank G. N. Gavrila for technical assistance with the MUSTANG endstation (Grant No. BMBF 05 KS40C1/3). We acknowledge the support through the EC under IA-SFS Contract No. RII 3-CT-2004-506008. Thanks are also due to the former Ministerio de Ciencia y Tecnología, Spain, for financial support through Projects No. TIC2002-04280-C03-03 and No. MAT05-04562 and to the Diputación General de Aragón (CAMRADS project).

*Present address: Centre d' Investigació en Nanociència i Nanotecnologia (CIN2-CSIC), Edifici CM-7, Campus de la UAB, E-08193 Bellaterra, Spain.

[1] D. Jérome, Science **252**, 1509 (1990).
[2] F. Mila and K. Penc, Synth. Met. **70**, 997 (1995).
[3] C. Bourbonnais and D. Jérome, Science **281**, 1155 (1998).
[4] T. Ishiguro, K. Yamaji, and G. Saito, *Organic Superconductors* (Springer, Berlin, 1998).
[5] M. Dumm, A. Loidl, B. W. Fravel, K. P. Starkey, L. K. Montgomery, and M. Dressel, Phys. Rev. B **61**, 511 (2000).
[6] P. Auban-Senzier and D. Jérome, Synth. Met. **133-134**, 1 (2003).
[7] T. Giamarchi, *Quantum Physics in One Dimension* (Oxford University Press, Oxford, 2004).
[8] J. Fraxedas, *Molecular Organic Materials: From Molecules to Crystalline Solids* (Cambridge University Press, Cambridge, England, 2006).
[9] P. Batail, K. Boubekeur, M. Fourmigué, and J.-C. P. Gabriel, Chem. Mater. **10**, 3005 (1998).
[10] K. Bechgaard, C. S. Jacobsen, K. Mortensen, H. J. Pedersen, and N. Thorup, Solid State Commun. **33**, 1119 (1980).
[11] B. Liautard, S. Peytavin, G. Brun, D. Chasseau, J. M. Fabre, and L. Giral, Acta Crystallogr., Sect. C: Cryst. Struct. Commun. **40**, 1023 (1984).
[12] S. Perruchas, J. Fraxedas, E. Canadell, P. Auban-Senzier, and P. Batail, Adv. Mater. (Weinheim, Ger.) **17**, 209 (2005).
[13] H. Kobayashi, A. Kobayashi, Y. Sasaki, G. Saito, and H. Inokuchi, Bull. Chem. Soc. Jpn. **57**, 2025 (1984).
[14] R. Moret and J. P. Pouget, in *Crystal Chemistry and Properties of Materials with Quasi-One-Dimensional Structures*, edited by J. Rouxel (Reidel, Dordrecht, 1986).
[15] F. Nad, P. Monceau, C. Carcel, and J. M. Fabre, Phys. Rev. B **62**, 1753 (2000).
[16] D. S. Chow, F. Zamborszky, B. Alavi, D. J. Tantillo, A. Baur, C. A. Merlic, and S. E. Brown, Phys. Rev. Lett. **85**, 1698 (2000).
[17] C. Coulon, P. Delhaes, S. Flandrois, R. Lagnier, E. Bonjour, and J. M. Fabre, J. Phys. (Paris) **43**, 1059 (1982).
[18] F. Nad, P. Monceau, C. Carcel, and J. M. Fabre, J. Phys.: Condens. Matter **13**, L717 (2001).
[19] C. Coulon, S. S. P. Parkin, and R. Laversanne, Phys. Rev. B **31**, 3583 (1985).
[20] H. H. S. Javadi, R. Laversanne, and A. J. Epstein, Phys. Rev. B **37**, 4280 (1988).
[21] S. S. P. Parkin, J. J. Mayerle, and E. M. Engler, J. Phys. (Paris), Colloq. **44**, C3-1105 (1983).
[22] T. Nakamura, T. Hara, and K. Furukawa, J. Low Temp. Phys. **142**, 629 (2006).
[23] J. Taborski, P. Väterlein, H. Dietz, U. Zimmermann, and E. Umbach, J. Electron Spectrosc. Relat. Phenom. **75**, 129 (1995).
[24] A. M. Bradshaw and N. V. Richardson, Pure Appl. Chem. **68**, 457 (1996).
[25] S. Ravy, P. Foury-Leylekian, D. Le Bolloc'h, J.-P. Pouget, J. M. Fabre, R. J. Prado, and P. Lagarde, J. Phys. IV **114**, 81 (2004).
[26] G. N. George and M. L. Gorbaty, J. Am. Chem. Soc. **111**, 3182 (1989).
[27] J. Fraxedas, Y. J. Lee, I. Jiménez, R. Gago, R. M. Nieminen, P. Ordejón, and E. Canadell, Phys. Rev. B **68**, 195115 (2003).
[28] C. Rojas, J. Caro, M. Grioni, and J. Fraxedas, Surf. Sci. **482-485**, 546 (2001).
[29] J. Fraxedas, A. Verdaguer, F. Sanz, S. Baudron, and P. Batail, Surf. Sci. **588**, 41 (2005).
[30] F. Zwick, S. Brown, G. Margaritondo, C. Merlic, M. Onellion, J. Voit, and M. Grioni, Phys. Rev. Lett. **79**, 3982 (1997).
[31] M. Sing, U. Schwingenschlogl, R. Claessen, M. Dressel, and C. S. Jacobsen, Phys. Rev. B **67**, 125402 (2003).
[32] The cooling rate is a very important factor when determining the transport properties of Bechgaard-Fabre salts and in general of

molecular organic materials. In the case of $(TMTSF)_2ClO_4$ single crystals the electrical conductivity increases below 24 K with the onset of anion-ordering when slowly cooled (about 0.1 K min^{-1}) and superconductivity appears at 1.2 K upon further cooling (*R* state). However, for rapid cooling (>50 K min^{-1}) the crystals exhibit a metal-insulator transition below 6 K (*Q* state). For details see, e.g., T. Takahashi, D. Jérome, and K. Bechgaard, J. Phys. (France) Lett. **43**, L565 (1982); H. Schwenk, K. Andres, and F. Wudl, Phys. Rev. B **29**, 500 (1984).

[33] J. J. Ritsko, N. O. Lipari, P. C. Gibbons, and S. E. Schnatterly, Phys. Rev. Lett. **37**, 1068 (1976).

[34] J. M. Soler, E. Artacho, J. D. Gale, A. García, J. Junquera, P. Ordejón, and D. Sánchez-Portal, J. Phys.: Condens. Matter **14**, 2745 (2002).

[35] No changes could be detected on preliminary F 1*s* XANES measurements performed on single crystals of $(TMTTF)_2PF_6$ across the charge-ordering transition under similar experimental conditions.

[36] R. Nyholm and N. Mårtensson, Phys. Rev. B **36**, 20 (1987).

[37] A. S. Y. Chan, G. K. Wertheim, H. Wang, M. D. Ulrich, J. E. Rowe, and T. E. Madey, Phys. Rev. B **72**, 035442 (2005).

[38] A. S. Coolidge, H. M. James, and R. D. Present, J. Chem. Phys. **4**, 193 (1936).

[39] The analysis of the S 2*p* and O 1*s* lines shows that the low-temperature spectra (116 K) are shifted about 0.1 eV toward higher binding energies as compared to the higher-temperature spectra (207 K). However, the uncertainty in the peak position is larger for both lines as compared to the Re 4*f* lines since they are broader and in the case of S 2*p* they have two signals arising from neutral and charged TMTTF. A detailed discussion on the deconvolution of S 2*p* lines from TMTTF-based and dithiolene-based materials can be found in pp. 72–73 of Ref. 8 and in I. Malfant, K. Rivasseau, J. Fraxedas, Ch. Faulmann, D. de Caro, L. Valade, L. Kaboub, Jean-Marc Fabre, and F. Senocq, J. Am. Chem. Soc. **128**, 5612 (2006).